Journal of Instrumentation

PAPER • OPEN ACCESS

Detection of warning signal of particulate emission on the basis of fixed threshold in real-time using a lidar system

J inst

Published by IOP Publishing for Sissa Medialab

Received: *December 14, 2022*
Revised: *March 28, 2023*
Accepted: *April 17, 2023*
Published: *May 5, 2023*

6TH International Conference Frontiers in Diagnostics Technologies
ENEA Frascati Research Centre, Frascati, Italy
19–21 October 2022

2023 JINST 18 C05006

Detection of warning signal of particulate emission on the basis of fixed threshold in real-time using a lidar system

N. Rutigliano,[*] L. Martellucci, A. Puleio, R. Rossi, I. Wyss and P. Gaudio

Industrial Engineering Department, Università degli Studi di Roma Tor Vergata, Via del Politecnico 1, 00133, Roma, Italy

E-mail: novella.rutigliano@alumni.uniroma2.eu

Abstract: Monitoring pollutant emissions in an urban area is of primary importance in order to guarantee high levels of human health (by reducing the impact of respiratory diseases on urban inhabitants) and good preservation of objects (such as historical sites or buildings). The European Environment Agency (EEA) has established that the maximum concentration of PM2.5 concentration for long-term exposure is 10 µg/m3. By measuring the light that has been backscattered by atmospheric particulates, the lidar technique seems to be a valid method to provide a warning signal when a particulate concentration threshold is exceeded. In addition, the lidar system can also provide information about the distance at which the particulate threshold is exceeded. In this research measurements of traffic-originated particulate in the area near the University of Rome "Tor Vergata" is analysed at different times on a weekday to obtain continuous monitoring of its backscattering coefficient, values of particulate concentration and details about time and distance from the lidar system at which a warning signal is provided. The University of Rome "Tor Vergata" is in an area where traffic is very heavy, so high pollutant concentration values are to be expected.

Keywords: Detector modelling and simulations I (interaction of radiation with matter, interaction of photons with matter, interaction of hadrons with matter, etc); Interaction of radiation with matter; Simulation methods and programs

[*]Corresponding author.

https://doi.org/10.1088/1748-0221/18/05/C05006

Contents

1 Introduction

The beginning of the 21st century has seen a growing awareness that human health goes hand in hand with environmental protection: monitoring the environment in which a human settlement is located therefore means monitoring the protection of the settlement itself.

What makes monitoring activities effective are the rapidity of detecting an alarm situation, the possibility of continuous measurements and the spatial extent of the area that can be monitored. With reference to these requirements, lidar technology seems to be very suitable to detect anomalies in the concentration of particulate matter in the atmosphere, particulate matter that could be toxic or carcinogenic to humans.

In the last decades, environmental monitoring and diagnostic with lidar systems have significantly grown. For what strictly concerns monitoring of urban pollutant emissions a lot of studies have been carried out in the investigated time scenario.

The main objectives of the studies concerning this application are to find out the characteristics ([1–3]) main emission sources ([1, 2, 4]) and spatial distribution ([5, 6]) of urban particulate matter.

The aim of the present study is to adopt a methodology to calibrate the lidar system used and to analyse the preliminary results obtained. The analysis provided in this work only relates to the notification of an exceedance of the backscattering coefficient threshold. This is because lidar systems in horizontal applications are not, in the present state of art, able to return an absolute value for the local atmospheric concentration, but they can only provide variations of signal intensity from a non-perturbated reference-taken signal. Our goal is to use the measurement of the variation of the backscattering signal as a concentration change that can provide an alarm. This makes it possible to have a system that can perform real-time monitoring in different environments (rural, industrial, forest, oceanic) and that can detect alarm conditions whenever there is an accidental emission of a gaseous substance or aerosols into the atmosphere without being able to classify the causes (this is due to the high sensitivity of lidar systems, but their low specificity). An example of use of lidar systems as alarm detection can be found in two different papers of Bellecci et al. [7] and Vilar et all [8] where the use of lidar as forest fire detection is has been proposed.

Two days of case study (in spring season) of environmental measurements have been conducted. Preliminary weather data have been considered for the final evaluation.

2 Materials and methods

2.1 Experimental apparatus

In figure 1 is reported the experimental apparatus used for the measurements.

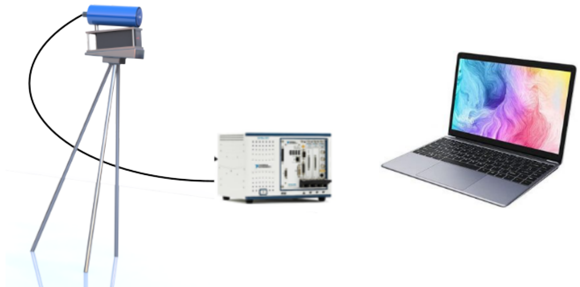

Figure 1. Experimental apparatus. From top-left clockwise: APD, telescope, laser source, pc, NI-PXI.

It is composed of a transmitter based on Nd:YAG laser source (1064 nm, 400 mJ, 10 Hz) and a receiver system constituted by a Cassegrain telescope (aperture: 102 mm, focal length: 1200 mm) and a silicon avalanche photodiode (Si-APD). Finally, the optical signal transduced into an electrical one is acquired and stored using an NI-PXI and a pc for the data analysis. NI-PXI is 10 bit, 100 Msps/s analog-to-digital converter. The system is located at a height of 15 m above the street level. The system was positioned at this height to ensure eye-safe conditions. More details on this aspect are reported in appendix A.

Figure 2. Map of the monitored zone. Maps Data: Google ©2023.

The monitored zone, reported in figure 2, can be schematically represented by an imaginary line connecting the Industrial Engineering department and the parking of the School of Economics. A further analysis has been carried out for a specific distance (170 m from the system) that corresponds to Via Cambridge: a heavy-traffic street between the School of Engineering and the School of Economics.

2023 JINST 18 C05006

The entire acquisition for the lidar system is described by the well-known elastic lidar equation of the backscattered power, which is reported here in equation (2.1)

$$P_b\left(\lambda, R\right) = \frac{C}{R^2}\beta_\pi\left(\lambda, R\right) e^{-2\int_o^R k(\lambda.R')dR'} . \tag{2.1}$$

C is a system constant, here evaluated using the algorithm proposed by Stelmaszczyk et al. in [9], R [m] is the range variable, β_π [m^{-1}] is the backscattering coefficient, λ is the wavelength of the laser beam, k [m^{-1}] is the extinction coefficient.

2.2 Preliminary data

To operate an inversion of the acquired data some preliminary information is required such as visibility, relative humidity and wind direction and intensity. These weather data are necessary because they behave as input parameters for reference values of backscattering coefficient and extinction coefficient proposed in [10] to be used in the inversion method, which will be described in section 2.3. Visibility gives us information about the extinction of a collimated light beam in a particular environment (by the definition of *visibility* given by the World Meteorological Organisation). From visibility, the extinction coefficient could be evaluated by equation (2.2) (as reported in [11])

$$k = \frac{3.91}{V}\left(\frac{\lambda}{0.55}\right)^{-q} . \tag{2.2}$$

Where k is the extinction coefficient [km^{-1}], V is the meteorological visibility [km^{-1}], λ is the wavelength of the light beam [µm] and q is an empirical coefficient depending on the range of visibility ($0.585V^{-1/3}$ if $6\,\text{km} \leq V$, 1.3 if $6\,\text{km} < V \leq 50\,\text{km}$ and 1.6 if $V > 50\,\text{km}$).

Relative humidity directly influences the optical properties of atmospheric particles because, as a result of the deposition of water on their surface, it increases their geometric cross-sectional area. These preliminary data have been downloaded from a weather forecast database and are reported in tables 1 and 2.

Table 1. Wind, relative humidity, and visibility for day 1 of the measurements for the hours of interest.

	Day 1		
	wind	RH [%]	VIS
9	NNE-4	66	good
10	NNE-4	57	good
11	NNW-3	50	good
12	WNW-7	44	good
13	WNW-5	62	good
14	WNW-8	62	good
15	W-7	62	good
16	W-4	71	discrete
17	SSW-4	76	good
18	S-4	81	good

2023 JINST 18 C05006

Table 2. Wind, relative humidity, and visibility for day 2 of the measurements for the hours of interest.

	Day 2		
	wind	RH [%]	VIS
9	W-12	62	good
10	W-15	61	good
11	W-6	57	good
12	NW-11	22	good
13	W-17	47	good

Visibility and relative humidity are dependent variables for the reference model of the aerosol optical properties of the lower atmosphere [10].

2.3 Methods

An experimental campaign has been conducted with the lidar system introduced in section 2.1. Once the raw data has been transferred from NI-PXI to the PC, they have been analysed. The analysis algorithm could be summarised as follows:

- Data normalisation and preprocessing operations (background subtraction, filtering)
- Evaluation of μ (range corrected signal) and SNR (signal-to-noise ratio)
- Assumption of β_π and k, optical reference value, from [10]
- Evaluation of β_π with Klett's method for the inversion
- Normalisation of the results obtained by the reference value of the backscattering coefficient to get percentage values of the threshold (taken as the reference value) exceeding.

Preliminary notes on calibration are necessary at this point in the discussion:

- The lidar system does not require quantitative calibration because the signal, via the PXI, is read in volts. In addition, a general quantitative calibration would not be necessary for the inversion method, which is based on relative values, considering that the lidar equation is an integral equation.
- For small distances, the geometric compression factor of the signal (which in the lidar equation is found in the constant C) turns out to be of paramount importance. Calibration of this parameter was carried out numerically by using the algorithm proposed by Stelmaszczyk et al. in [9].
- For the other acquisition parameters, however, which more properly concern the experimental setup, numerical simulations were first carried out to identify the range of visibility of the signal, then validated with experimental measurements prior to the campaign presented here.

2023 JINST 18 C05006

The inversion method used is the one proposed by Klett in [12] for a non-homogeneous atmosphere. It assumes that a certain reference value is known at a fixed point, and it is used as a boundary condition. In our case, the reference value has been taken as β_π at the reference distance of 1,5 m (This assumption is not highly simplifying because, if I fix the reference point close enough to the system, I can observe for myself whether or not there are anomalous conditions with respect to the unperturbed conditions whose constants have been tabulated in [10]). By applying this method, the backscattering coefficient is evaluated as follows:

$$\beta_\pi = \frac{e^{(\mu-\mu)}}{\frac{1}{\beta_\pi} + \frac{2}{P}\int_R^R e^{(\mu-\mu)}\,dR'}\,. \tag{2.3}$$

Where new variables introduced, R and P are, respectively, the reference distance (1.5 m) and the ratio of extinction coefficient and backscattering coefficient calculated at the reference distance.

Since lidar gives back non-absolute values, but the possibility to quantify a comparison between the observed value and a threshold (here assumed as the non-perturbated value taken from [8]), all the results will be presented as a ratio between the backscattering coefficient obtained as an output from the Matlab code and the reference one for an urban environment with a specific RH (Relative Humidity). This normalization, by evaluating the ratio between the backscattering coefficient obtained with the inversion algorithm and the reference value of a non-perturbated atmosphere scenario, is useful to underline the level of threshold exceeding. This exceeding could be easily referred as a signal 'alarm' condition.

Lidar is not able to clearly define the phenomenon that originated a variability in the local atmospheric concentration, but since we were observing a street, we can say with a certain level of confidence that the anomalies on the lidar signal are due to urban traffic.

At the end, we compared information about the wind and the fluid dynamics of the plume.

Uncertainty analysis was conducted by evaluating the percentage standard deviation of 100 pulses for the same measurement. The error committed in this way is approximately 15%.

3 Results and Conclusions

The results are presented in two different ways: a contour map of a time evolution along the special range of the normalised backscattering coefficient (figure 3) and a time evolution at a fixed distance for the same parameter (figure 4).

The first type of graph proposed is interesting because it is able to show a graphical relationship between the area where the atmospheric density is locally altered and the wind direction and intensity. With lidar technology, we are not able to derive the nature of the local variation in atmospheric density from the measurements. Considering a source of particulate matter emitting into the atmosphere, a local density change is observed in the region where this occurs. This region, when crossed by a laser beam, gives rise to a visible increase in the lidar signal. The sensitivity of lidar technology to local density variation is very high, but, due to what has just been said, not very specific. To understand the cause of the observed variation, it is therefore necessary to integrate the lidar system with other technologies (such as chemical sensors implemented on mobile devices).

2023 JINST 18 C05006

The intended use of systems such as the one preliminarily studied in this paper concerns continuous monitoring capable of providing alarm detection. The alarm is thus given when the quantity under consideration exceeds a value set as a threshold value.

This type of graph gives information on the portion of the monitored area affected by the local variation in atmospheric density.

The second type of graph, on the other hand, is interesting because, by limiting the representation of the ratio trend in question to a single fixed distance (equal to the centreline of Via Cambridge), it gives an indication of the extent to which the value obtained for the backscattering coefficient exceeds the value taken as a reference.

In figure 3 is presented the time evolution map of the ratio $\frac{\beta_\pi}{\beta_{\pi^*}}$ and the information for the wind direction. On the x axis it is reported the time [hh:mm] of measurement, while on the y axis the distance [m]. The intensity of the colour map (whose legend is reported on the side of each graph) represents the intensity value of the ratio.

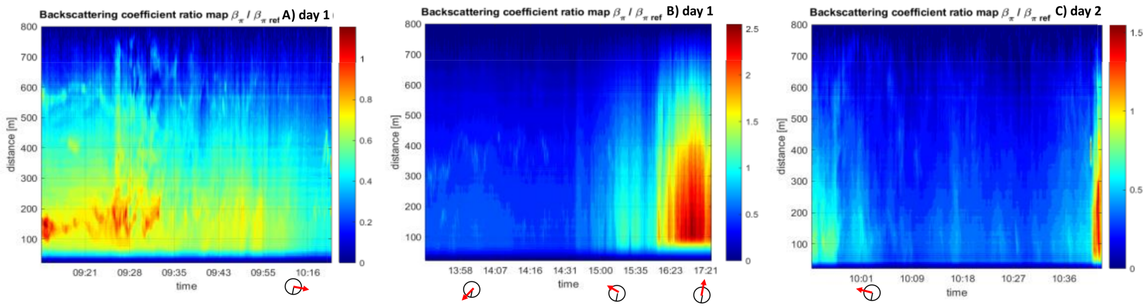

Figure 3. Time evolution map for the ratio during A) the morning of the first day of measurements, B) the afternoon of the first day and C) the morning of the second day. Schematic representation of the wind direction is reported under the time axis.

We observe an higher value of the ratio during three different time windows of the day: between 9.15 and 9.30 (which is just before the time start of first classes in the morning either in Economics School either in Engineering School), just before 11.00 a.m. (starting time of second classes and is approximately the most common hour at which university workers start their day) and between 16.30 and 17.30 (which is the finish time either for classes either for workers).

For what concerns information given by the wind we observe that in the E-W direction (which is perpendicular to the laser beam of the system presented here) we don't have influences on the backscattering coefficient all along the distance range analysed. While, for what concerns wind pointing to the south we have a spread of the plume all along the range direction and the anomaly is detected for almost 300 m and it is clearly represented by the rising in intensity of the red colour in the map.

In figure 4 is reported the time evolution of the ratio $\frac{\beta_\pi}{\beta_{\pi^*}}$ at a fixed distance (170 m) from the system corresponding to Via Cambridge.

Figure 4 is a focus on what happens on Via Cambridge during the period investigated. Time evaluations made for figure 3 are validated in figure 4: we have stronger exceeding of the reference threshold before the beginning of the working or lesson time and after its end. In this case, by referring to a fixed distance (which means a fixed point by considering that the entire range of analysis has been, in first approximation, described as a line), wind information gives no further interpretation of the phenomenon observed.

2023 JINST 18 C05006

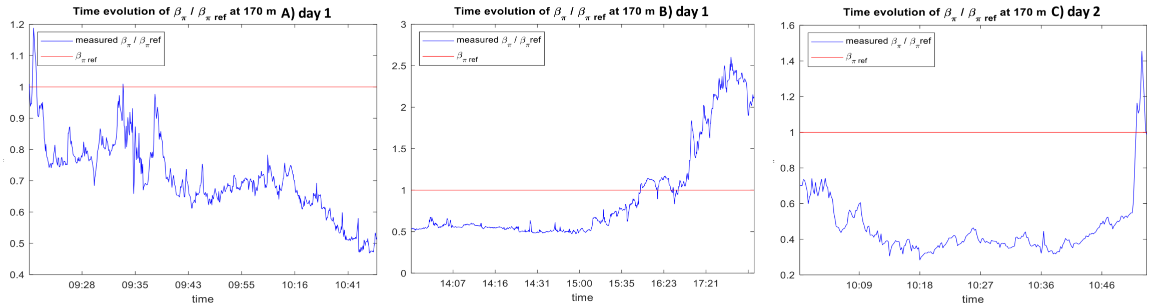

Figure 4. Time evolution at a fixed distance for the ratio into account during A) the morning of the first day of measurements, B) the afternoon of the first day and C) the morning of the second day. Schematic representation of the wind direction are reported under the time axis.

In conclusion, results presented in this work regarding preliminary tests with a lidar system as the one described in section 2 in terms of alarm detection of a backscattering threshold exceeding are based on the assumption that reference values for both backscattering and extinction coefficient are taken from [10] and only depends on relative humidity and visibility. By considering that our reference method is based on observation conducted in 1975 and that urban environment is supposed to have become significantly different in last fifty years, the accuracy of the reference values for backscattering and extinction coefficients must be increased. It should be interesting also to express a correlation between the two optical coefficients and temperature: this is because local variation of temperature is strongly related to a local variation of density which is exactly what lidar system is able to observe. Further studies will be conducted to collect more data, to create a database for reference values and to correlate different weather data to backscattering and extinction coefficient to have, depending on weather condition, a prediction on the value to be used as a reference one in the inversion equation.

A Demonstration of eye-safety conditions for current application

In this appendix eye-safety conditions under which the experimental campaign has been operated will be demonstrated.

The centreline of the laser head is positioned 15 m over the street level. At the exit, the spot of laser beam has a d_0 (5 mm) diameter and it's characterized by a divergence δ equal to 5 mrad. The aim of this appendix is to show that, although the laser beam can reach, due to its strong divergence, the eye level of human beings in transit on the road, the energy (and, most of all, the fluence) possessed by the beam in the conditions in which it intercepts human eyes and skin, is well below the limits sanctioned by law (in Italy D. Lgs 81/2008 and D.Lgs 106/2009). The quantity of interest, therefore, turns out to be the energy (normalised per unit area), absorbed by the biological matter (in this specific case the ocular retina since there is no danger to the skin).

By considering the divergence of the laser beam, the limit condition for fluence H [J/m^2] and for irradiance E [W/m^2] given by Italian law (respectively equal to 0,02 J/m2 and 23,64 W/m2 for a train of pulses) is reached at a horizontal distance of 300 m from the laser source. At this distance the laser beam has a fluence of 0,019 J/m^2 and an irradiance of 0,39 W/m^2. At such a distance from the laser head, we have no interaction between laser beam and people walking on the street (laser beam diameter is 5 m).

It is necessary to underline that such a system presented in section 2 is a prototype, but our aim is to develop a system with a laser beam with less pulse energy (0,05 J). This data influences the eye-safety distance by reducing this parameter to 170 m.

Acknowledgments

The present work is a preliminary study for the implementation of a lidar system for the project PIA SENSOR — Code 7LZ5BJ7 — CUP B91B21006390007 in collaboration with TAAL s.r.l.

References

[1] H. Panahifar, R. Moradhaseli and H.R. Khalesifard, *Monitoring atmospheric particulate matters using vertically resolved matters using vertically resolved lidar, in-situ recordings and satellite data over Tehran, Iran*, Sci. Rep. **10** (2020) 20052.

[2] F. Lisetskii and A. Borovlev, *Monitoring of Emission of Particulate Matter and Air Pollution using Lidar in*, Aerosol Air Qual. Res. **19** (2019) 504.

[3] A. Wiedensohler et al., *Black carbon emission and transport mechanisms to the free troposphere at the La Paz/El Alto (Bolivia) metropolitan area based on the Day of Census (2012)*, Atmos. Environ. **194** (2018) 158.

[4] Y. Yang et al., *Characteristics of Heavy Particulate Matter Pollution Events Over Hong Kong and Their Relationships With Vertical Wind Profiles Using High-Time-Resolution Doppler Lidar Measurements*, J. Geophys. Res. Atmos. **124** (2019) 9609.

[5] L. Lv, T. Zhang, Y. Xiang, W. Chai and W. Liu, *Distribution and transport characteristics of fine particulate matter in beijing with mobile lidar measurements from 2015 to 2018*, J. Environ. Sci. **115** (2022) 65.

[6] T.D. Toth et al., *Retrieving particulate matter concentrations over the contiguous United States using CALIOP observations*, Atmos. Environ. **274** (2022) 118979.

[7] C. Bellecci et al., *Application of a CO_2 dial system for infrared detection of forest fire and reduction of false alarm*, Appl. Phys. B **87** (2007) 373.

[8] R. Vilar and A. Lavrov, *Estimation of required parameters for detection of small smoke plumes by lidar at 1.54* µm, Appl. Phys. B **71** (2000) 225.

[9] K. Stelmaszczyk et al., *Analytical function for lidar geometrical compression form-factor calculations*, Appl. Opt. **44** (2005) 1323.

[10] E.P. Shettle and R.W. Fenn, *Models for the aerosols of the lower atmosphere and the effects of humidity variation on their optical properties*, AFGL-TR-79-O214, *Environ. Res. Papers*, no. 676 (1979) [https://apps.dtic.mil/sti/pdfs/ADA085951.pdf].

[11] R.M. Measures, *Laser Remote Sensing: searchlight on the environment*, Endeavour **13** (1989) 108.

[12] J.D. Klett, *Stable analytical solution for processing lidar returns*, Appl. Opt. **20** (1981) 221.